Geologia Croatica	66/3	233–244	9 Figs.	2 Tabs.		Zagreb 2013

Development of framboidal pyrite in the Upper Permian marly limestone of the NE-Hungarian Darnó Hill

Gabriella B. Kiss[1] and Federica Zaccarini[2]

[1] Department of Mineralogy, Eötvös Loránd University, H-1117 Budapest, Pázmány P. stny. 1/c, Hungary; (gabriella-kiss@chello.hu)

[2] Department of Applied Geosciences and Geophysics, University of Leoben, A-8700 Leoben, Peter Tunner str. 5, Austria

doi: 10.4154/gc2013.19

Geologia Croatica

ABSTRACT

The NE Hungarian Darnó Hill is geologically complex; it is composed of an accretionary mélange complex, which contains Permian, Triassic and Jurassic sedimentary and magmatic blocks. The succession can easily be correlated with the NW Dinarides, using evidences of the different evolutionary stages of the Neotethyan Ocean (rifting, marginal basin opening, closure). Several ore indications are known from this area, but their genesis is poorly understood, mostly because of the complexity of the geological structures. The present study deals with one of these indications from deep drilling. A framboidal pyrite bearing Permian-Triassic marly limestone series was investigated, which was previously described as a possible analogy of the Polish-German copper shales (Kupferschiefer). Framboidal pyrite, euhedral pyrite overgrowths (both with high Au content), disseminated euhedral and anhedral pyrite (without overgrowth), anhedral chalcopyrite, galena and sphalerite were recorded by detailed microscopy, EPMA and whole rock geochemical analyses. There is a slightly enriched total metal content of 100-200 ppm in the mineralized sediments compared to the unmineralized ones. The minerals formed under reducing, anoxic, marine sedimentary conditions, in several steps; during synsedimentary, early diagenetic and epigenetic processes. The characteristics confirmed by the research are typical of the weakly mineralized Kupferschiefer type.

Keywords: Weakly mineralized Kupferschiefer type, Permian-Triassic sediments, framboidal pyrite, euhedral pyrite overgrowth, micrograins of chalcopyrite, sphalerite and galena

1. INTRODUCTION

Several different mineralizations, such as native copper bearing calcite-zeolite veins and chalcopyrite bearing quartz-prehnite veins in basalt, exhalative iron ore and a copper shale indication have been documented in the restricted 10 km^2 area of Darnó Hill (Fig. 1.) (HAIDINGER, 1850, MEZŐSI & GRASSELLY, 1949, KISS, 1958, BAKSA et al., 1981, MOLNÁR & KISS, 2013). The genesis of the ore indications is mostly unclear due to the rather complex geology.

A geological correlation has recently been established between Darnó Hill and the NW Dinarides, based on stratigraphic, mineralogical and petrological data, as well as research on the tectonic evolution of the region. According to DIMITRIJEVIĆ et al. (2003), HAAS & KOVÁCS (2001), KOVÁCS et al. (2008, 2010), HAAS et al. (2011) and KISS et al. (2008, 2010, 2012), the Permian, Triassic and Jurassic sedimentary rocks, together with the Triassic and Jurassic submarine basalts of Darnó Hill, form a Neotethyan accrétionary mélange complex, which was displaced from the Dinarides to NE Hungary along the Mid-Hungarian Lineament.

The recently accepted geological model has provided a reliable structural framework, within which the host rock sequence can be interpreted, focusing on the ore mineralization. The present study deals with the framboidal pyrite bearing copper shale indication, in order to provide geochemical and mineralogical data in this poorly studied mineralization, with the ultimate aim of providing more information regarding ore genesis.

2. GEOLOGICAL BACKGROUND

Darnó Hill (Fig. 1) is part of the Darnó Unit, a part of the Bükk Unit, within the Pelso Unit of the ALCAPA Block (ALpine, CArpathian, PAnnonian, CSONTOS, 1995, SCHMID et al., 2008). According to the latest tectonic models, the Darnó Unit is the uppermost of four knappes, which compose the Bükk Unit. The lowest unit is the „Bükk Parautochton", which contains Palaeozoic to Jurassic formations. The Mónosbél Unit, above it, is mainly composed of Jurassic redeposited slope sediments. The Szarvaskő Unit contains an incomplete Jurassic, back-arc-basin or marginal basin opening related ophiolite-like sequence associated with deep-sea sediments. The Darnó Unit is made up of Triassic, Neotethyan rifting related and Jurassic, back-arc-basin opening related submarine volcanites and associated sedimentary rocks. These rocks form blocks in an accrétionary mélange complex of Neotethyan origin. According to the latest tectonic models, the Bükk Unit can be correlated with the NW Dinarides (AIGNER-TORRES & KOLLER, 1999, CSONTOS, 1995, CSONTOS, 1999, DIMITRIJEVIĆ et al., 2003, HAAS & KOVÁCS, 2001, HARANGI et al., 1996, KOVÁCS et al., 2008, KISS et al., 2010, 2012).

Deep drilling performed in 1977–78 revealed that two of the aforementioned units are present in the area of the Darnó Hill; the deeper positioned Mónosbél Unit and above it, the Darnó Unit (HAAS & KOVÁCS, 2001, KOVÁCS et al., 2008). Among the slope sediments of the Mónosbél Unit, Upper Permian – Lower Triassic shale-limestone blocks as well as Triassic Neotethyan rifting related peperitic basalt blocks (similar to the ones found in the Darnó Unit) are observed (ORAVECZ, 1978, KOVÁCS et al., 2008, KISS et al., 2010). The two units are partly covered by Oligocene sedimentary rocks, Miocene volcanites and sedimentary rocks, and with Quaternary cover (FÖLDESSY, 1975).

The studied mineralization was discovered in two 1200 m deep cores (RM-131 and RM-135, Fig. 1.), at the depth of 920-1050 m, in the Mónosbél Unit, when the drillcores were assayed in 10 m composite samples (BAKSA et al. 1981). In both cases, copper enrichment was found in Upper Permian – Lower Triassic limestone with shale intercalations, characterized by their high content of organic material. In the RM-131 core, the highest copper concentrations were between 930 and 940 m, but elevated values were observed from 890-990 m. The 0.1-0.28% Cu content was attributed to chalcopyrite found on the rims of pyrite of bacterial origin. Thus, the indication was interpreted as an analogue of the *Kupferschiefer* deposits (i.e. black-shale hosted synsedimentary copper deposit), though several questions concerning the mineral paragenesis and the geochemistry remained unanswered (BAKSA et al., 1981).

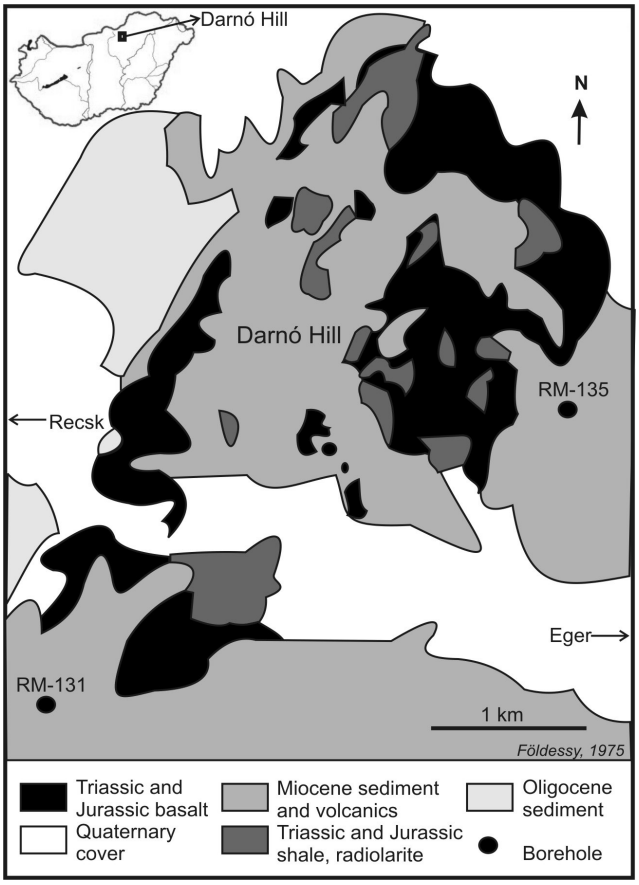

Figure 1: Geological map of Darnó Hill. The location of the studied drilling (RM-131) and additional drilling, in which similar mineralization was localized (RM-135) are also shown.

METHODS

The studied 120 m deep RM-131 borehole was drilled in 1977–78 on the southern part of the Darnó Hill, in the framework of the structural geological research of the nearby Recsk area. In the progress of this research, a 100m long part of the drillcore (900-1000 m) was studied in detail. Below the strongly sheared zone, (from 900 m to 928 m), marly limestone with shale intercalations was detected. Below this unit, from 990 m, there is a strongly tectonized zone.

Samples representing the typical features of all three units were studied in detail by microscopy (from 910.5 m, 912.8 m, 933.0 m, 950.0 m, 962.0 m, 965.4 m and 996.7 m). Petrography of the samples with emphasis on the ore minerals was undertaken on polished thin sections.

Electron microprobe analyses were used to characterize the composition of the different types of pyrite crystals and overgrowths, chalcopyrite and sphalerite grains, and to obtain elemental maps of the framboidal pyrite and the euhedral pyrite aggregates. This study was undertaken at the Eugen Stumpfl Laboratory of the University Centre of Applied Geosciences (University of Leoben, Austria), where a Superprobe Jeol JXA 8200 instrument was used in WDS mode, with 20 kV accelerating voltage and 10 nA beam current. The beam diameter was about 1 μm. The X-ray lines used were: Kα for S, Fe, Co, Zn, Cu and Ni; Lα for Te, Ag, Sb, Se and As; Mα for Au and Pb. The following diffracting crystals were selected: PETJ for S, Sb, Pb, Ag, Au and Te, LIFH for Cu, Fe, Zn, Ni and Co and TAP for As and Te. The counting time for peak and both backgrounds (left and right) were 20 and 10 seconds respectively. Synthetic NiS, Au-Ag alloy, $AgBiSe_2$, PdSb and Bi_2Te_3, and natural pyrite, chalcopyrite,

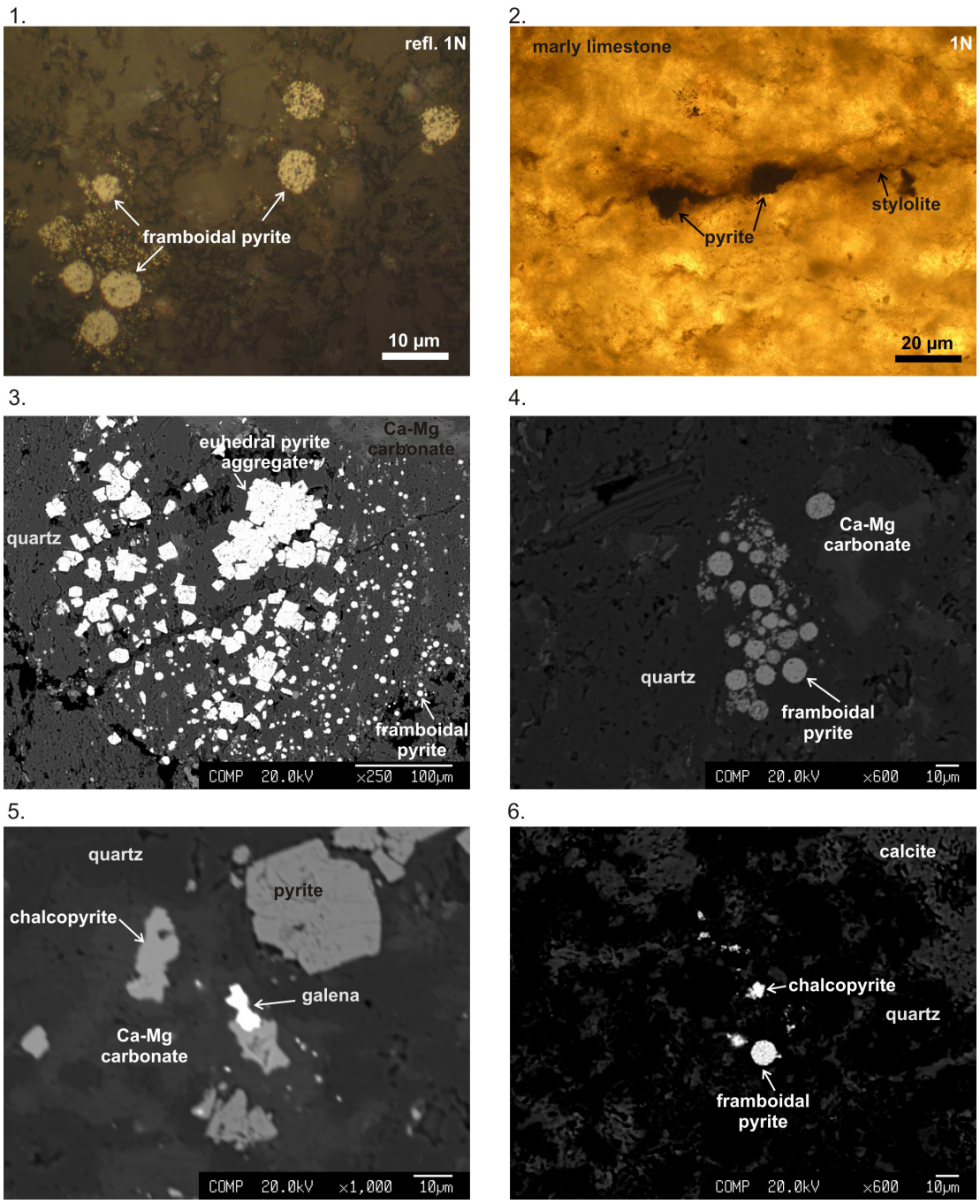

Figure 2: Opaque minerals in the marly limestone. 1: Framboidal pyrite (950 m, reflected light, 1N). 2: Anhedral pyrite occurring along a stylolite in the marly limestone (950 m, 1N). 3: Framboidal pyrite occurring together with euhedral pyrite overgrowths in the quartz and Ca-Mg carbonate formed host rock (965.4 m, composite image, EPMA). 4: Framboidal pyrite occurring in the silicified marly limestone (962 m, composite image, EPMA). 5: Disseminated chalcopyrite and galena occurring together with a euhedral pyrite aggregate (962 m, composite image, EPMA). 6: Framboidal pyrite occurring together with fine-grained chalcopyrite and pyrite (962 m, composite image, EPMA).

sphalerite, galena, skutterudite and niccolite were used as standard. The detection limits were as follows: 180 ppm for Fe and Co (Co only for euhedral overgrowths sample 1-5, framboids sample 1-9 and chalcopyrite sample 1), 200 ppm for Ni, 250 ppm for Cu, 280 ppm for Te, 300 ppm for S and Zn, 350 ppm for Ag, 390 ppm for Sb, 400 ppm for Se, 620 ppm for Au, 700 ppm for As and 1100 ppm for Pb, 1400 ppm for Co (euhedral overgrowths sample 6-10, framboids sample 10-14, chalcopyrite sample 2-4, euhedral pyrite and sphalerite measurements). The same analytical conditions were used to obtain the X-ray elemental distribution maps.

Whole rock geochemical analyses of 3 samples, each representing 10-20 cm long sections of the drillcore, were made in the laboratory of the Hungarian Geological and Geophysical Institute. ICP-OES was used for major (Al_2O_3, BaO, CaO, Fe_2O_3, K_2O, MgO, MnO, Na_2O, P_2O_5, SiO_2, SO_3, SrO and TiO_2) and some of the trace element analysis (Co, Cr, Cu, Ni, V, Zn). ICP-MS was utilised for other trace elements

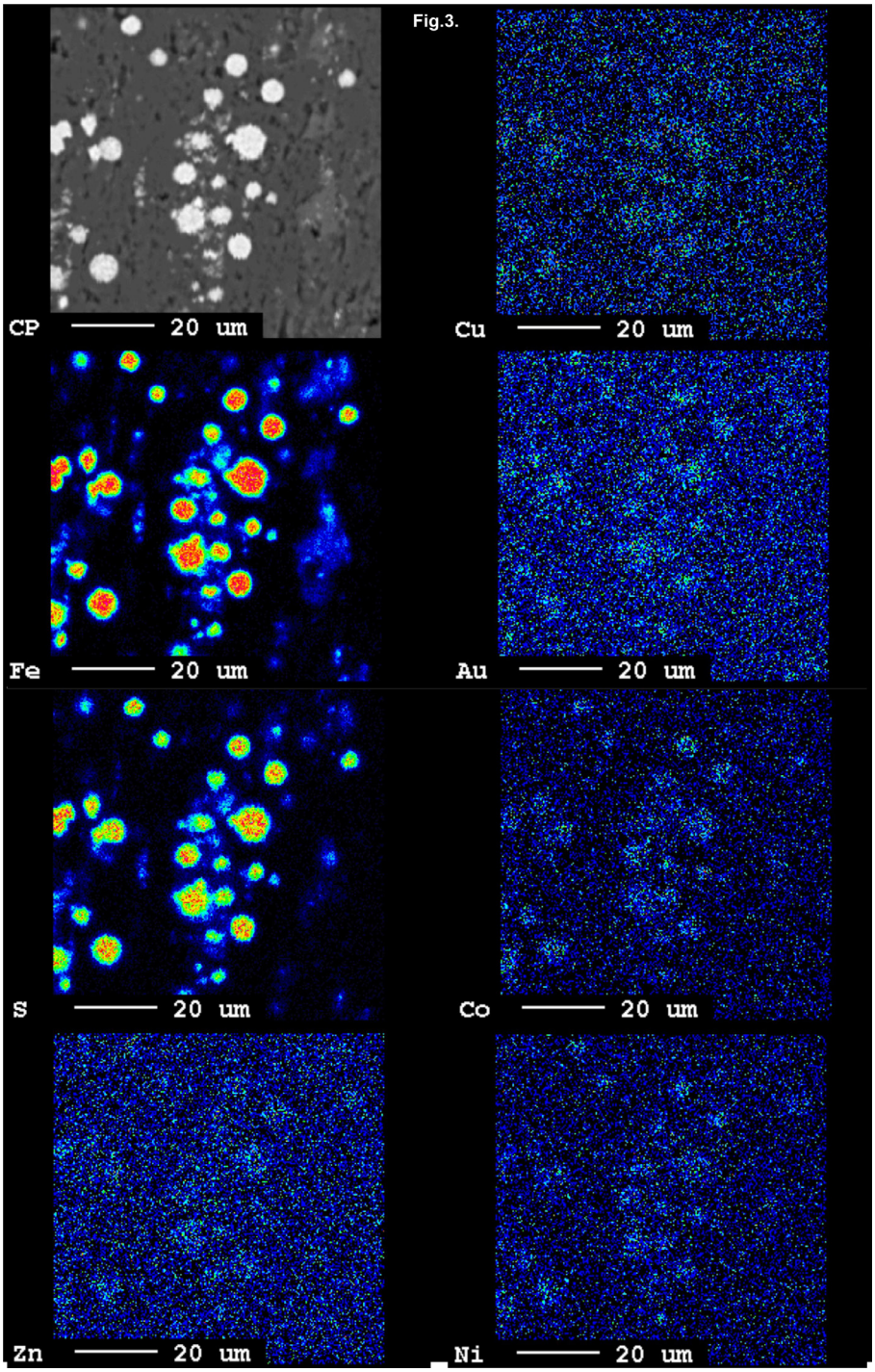

Figure 3: X-ray elemental distribution maps of framboidal pyrite (Cu, Fe, Au, S, Co, Zn, Ni). Compared to the euhedral pyrite overgrowths, it has a slightly higher Cu, Zn and Ni content.

(As, Rb, Y, Zr, Nb, Mo, Ag, Cd, Sn, Sb, Cs, La, Ce, Pr, Nd, Sm, Eu, Gd, Tb, Dy, Ho, Er, Tm, Yb, Lu, Hf, Ta, W, Tl, Pb, Bi, Th, U, PGE, Au, Te and W). Lithium borate and aqua regia digestion were used in preparing the samples. The detection limits for the major elements were between 0.0002 % (SrO) and 0.2 % (K_2O), while for the trace elements it was between 0.05 ppm and 1 ppm (0.05 ppm - Te, PGE; 0.1 ppm - Zn, Cd, Tl, REE; 0.2 ppm - Cu, Ag; 0.25 ppm - Mo, Bi, W, U, Th, Ta, Cs, Rb, Nb; 0.4 ppm - Ni; 0.5 ppm - Hf, Sn, Y, Zr; 0.6 ppm - As, Pb, Se; and 1 ppm - Li, V, Sb).

4. RESULTS

4.1. The host rock

The 100 m studied section of the drillcore is fairly uniform, regarding the rock type. It is composed of marly limestone with shale intercalation and shale beds. The upper part of the studied section, from 900–928 m, is strongly sheared, similarly to the lower part, from 990–1000 m. In spite of this, both zones contain the same rock types. Between these two

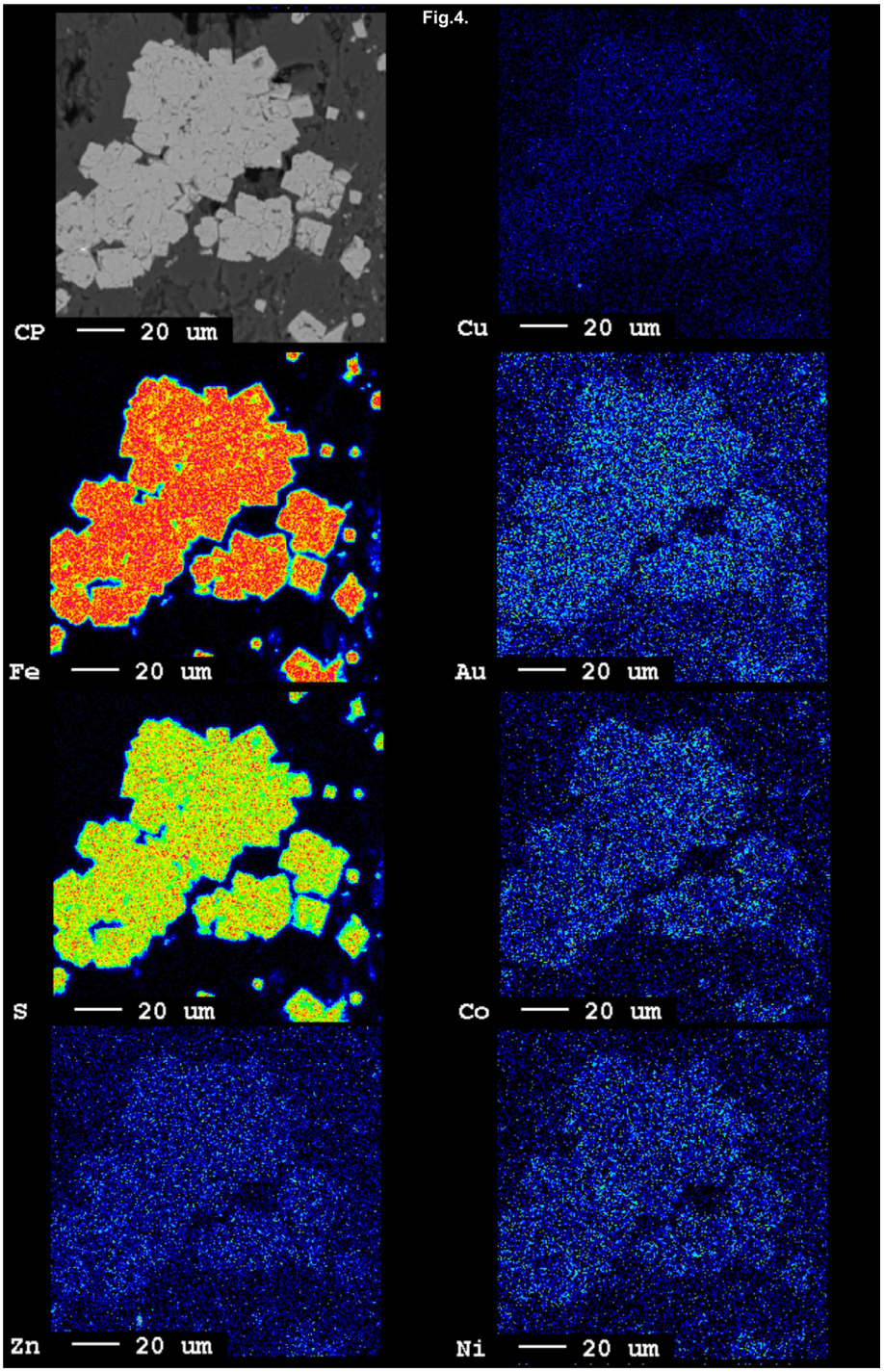

Figure 4: X-ray elemental distribution maps of the euhedral pyrite overgrowths (Cu, Fe, Au, S, Co, Zn, Ni). It has practically no Cu content, but compared to the framboidal pyrite, significantly more Au occurs.

tectonized zones, the rock is well preserved. The mineralization occurs in the latter unit.

The marly limestone is light grey coloured, at places stylolitic, and is cross-cut by 0.5–3 mm thick calcite veins. In thin section, a mixture of 50–200 μm sized patches, composed of calcite, quartz, rare ferro-dolomite and clay minerals, have been observed. The patches either contain a very fine grained mixture of all these minerals, or can be composed exclusively of calcite or quartz. In some cases, quartz displaces the aforementioned structures, thus later silicification of the marly limestone can be concluded. Rare muscovite, zircon, titanite, albite and apatite with a size variable from 10 to 100 μm were also recognized.

At least 3 vein generations can be distinguished; the older ones are filled mostly with spongy calcite, while the younger ones are more transparent, and can contain not only calcite, but also a small amount of quartz, dolomite and rare opaque minerals.

The shale intercalations in the marly limestone are dark grey to black in colour, and vary in thickness from 1–2 cm to several tens of centimetres. In general, this rock is strongly tectonized.

4.2. The ore minerals

Framboidal pyrite is the most abundant ore mineral in the studied samples (Fig. 2/1, 3, 4, 6). The framboids are 5–15 μm in size, and are composed of pyrite microcrystals (<1 μm diameter). These spherical phenomena fit well into the framboid definition of OHFUJI & RICKARD (2005). The framboids are disseminated in the marly limestone, with no relation to the stylolites or bedding. The EPMA analyses revealed that the framboidal pyrite is fairly rich in trace elements. Besides the quite common As (up to 0.356 mass%) and Ni (up to 0.62 mass%), Ag, Au, Co, Cu, Pb, Sb, Se and Zn occur also in some samples (0.027–3.212 mass%) (Table 1.). The X-ray elemental distribution mapping shows, that these trace elements are distributed uniformly over the framboids (Fig. 3.).

Euhedral pyrite overgrowths on framboidal pyrite form aggregates disseminated in the marly limestone (Fig. 2/3, 5). The size of the aggregates is between 25 μm - 80 μm, while single pyrite crystals can reach 10 μm. Based on the EPMA analyses, the pyrite of the aggregates is generally less enriched in trace elements, compared to the framboidal pyrite (e.g. As up to 0.263 mass%, Ni up to 0.043 mass%, and Cu, Pb, Zn, Se do not occur, or are not common) (Table 1.). How-

Table 1: Composition of the different ore minerals, based on the EPMA measurements.

	Sample	Fe	Co	Ni	Cu	Zn	Ag	Au	Pb	S	As	Se	Sb	Te	Total
Euhedral pyrite overgrowths on framboids (aggregates)	1	47.051	0.086	0.043	b.d.l.	b.d.l.	0.064	b.d.l.	b.d.l.	53.849	0.129	b.d.l.	0.05	b.d.l.	101.33
	2	46.752	0.084	0.024	b.d.l.	b.d.l.	b.d.l.	0.062	b.d.l.	53.937	b.d.l.	b.d.l.	b.d.l.	0.076	100.967
	3	47.059	0.066	b.d.l.	b.d.l.	b.d.l.	b.d.l.	b.d.l.	b.d.l.	53.889	0.124	b.d.l.	b.d.l.	b.d.l.	101.139
	4	46.411	0.151	0.022	b.d.l.	b.d.l.	b.d.l.	b.d.l.	b.d.l.	53.241	0.37	b.d.l.	b.d.l.	0.052	100.302
	5	46.689	0.069	b.d.l.	b.d.l.	b.d.l.	b.d.l.	0.067	b.d.l.	53.136	0.263	b.d.l.	0.043	b.d.l.	100.29
	6	47.756	b.d.l.	b.d.l.	b.d.l.	b.d.l.	b.d.l.	0.156	b.d.l.	53.400	b.d.l.	b.d.l.	b.d.l.	b.d.l.	101.323
	7	48.291	b.d.l.	b.d.l.	b.d.l.	b.d.l.	b.d.l.	b.d.l.	b.d.l.	53.696	b.d.l.	b.d.l.	b.d.l.	b.d.l.	102.128
	8	47.819	b.d.l.	b.d.l.	b.d.l.	b.d.l.	0.035	0.107	b.d.l.	53.589	b.d.l.	b.d.l.	b.d.l.	b.d.l.	101.583
	9	46.162	b.d.l.	0.027	b.d.l.	b.d.l.	0.055	b.d.l.	b.d.l.	52.032	b.d.l.	b.d.l.	b.d.l.	b.d.l.	98.355
	10	47.688	b.d.l.	b.d.l.	0.046	0.034	b.d.l.	b.d.l.	b.d.l.	53.689	b.d.l.	b.d.l.	b.d.l.	b.d.l.	101.471
Framboidal pyrite	1	45.718	0.332	0.296	0.044	b.d.l.	b.d.l.	b.d.l.	0.401	51.765	0.259	b.d.l.	b.d.l.	b.d.l.	98.824
	2	45.687	0.22	0.066	0.027	0.027	b.d.l.	b.d.l.	b.d.l.	52.444	0.356	b.d.l.	b.d.l.	b.d.l.	98.934
	3	46.988	0.183	0.051	0.042	b.d.l.	0.091	b.d.l.	b.d.l.	53.035	0.249	b.d.l.	b.d.l.	0.034	100.716
	4	45.967	0.192	0.093	b.d.l.	b.d.l.	b.d.l.	b.d.l.	0.221	52.431	0.253	b.d.l.	b.d.l.	b.d.l.	99.157
	5	46.301	0.189	0.088	b.d.l.	b.d.l.	b.d.l.	b.d.l.	b.d.l.	52.819	0.182	b.d.l.	b.d.l.	0.041	99.636
	6	46.366	0.202	0.079	b.d.l.	b.d.l.	b.d.l.	0.067	b.d.l.	52.725	0.134	b.d.l.	b.d.l.	b.d.l.	99.714
	7	46.358	0.204	0.072	0.03	b.d.l.	0.044	b.d.l.	b.d.l.	52.127	0.073	b.d.l.	b.d.l.	0.027	98.954
	8	46.686	0.172	0.052	b.d.l.	0.031	b.d.l.	0.067	b.d.l.	52.221	0.243	b.d.l.	0.053	0.029	99.707
	9	44.423	0.18	b.d.l.	0.037	b.d.l.	b.d.l.	b.d.l.	0.265	48.561	0.172	b.d.l.	b.d.l.	b.d.l.	93.668
	10	45.586	b.d.l.	0.039	b.d.l.	b.d.l.	b.d.l.	b.d.l.	b.d.l.	52.665	b.d.l.	b.d.l.	b.d.l.	b.d.l.	98.308
	11	43.897	b.d.l.	0.093	0.219	b.d.l.	b.d.l.	0.087	b.d.l.	48.612	0.077	0.069	0.031	b.d.l.	93.121
	12	43.68	4.536	0.36	1.115	b.d.l.	b.d.l.	b.d.l.	b.d.l.	49.261	0.097	b.d.l.	b.d.l.	b.d.l.	99.744
	13	44.896	b.d.l.	0.135	3.212	0.026	0.087	b.d.l.	b.d.l.	51.002	0.319	b.d.l.	0.046	b.d.l.	100.176
	14	44.762	b.d.l.	0.621	0.262	b.d.l.	0.044	b.d.l.	b.d.l.	52.52	0.169	b.d.l.	0.04	b.d.l.	98.507
Euhedral pyrite	1	46.178	b.d.l.	b.d.l.	0.03	b.d.l.	b.d.l.	b.d.l.	0.335	51.298	2.065	b.d.l.	b.d.l.	b.d.l.	99.956
Chalcopyrite	1	29.45	0.041	b.d.l.	34.494	b.d.l.	b.d.l.	b.d.l.	b.d.l.	34.019	b.d.l.	b.d.l.	b.d.l.	b.d.l.	98.103
	2	30.156	b.d.l.	b.d.l.	34.379	0.047	0.053	b.d.l.	b.d.l.	33.921	b.d.l.	b.d.l.	b.d.l.	b.d.l.	98.556
	3	29.824	b.d.l.	b.d.l.	33.083	0.03	b.d.l.	0.102	b.d.l.	35.247	b.d.l.	b.d.l.	b.d.l.	b.d.l.	98.32
	4	33.755	b.d.l.	0.062	21.804	0.043	b.d.l.	0.12	0.139	38.746	b.d.l.	0.04	b.d.l.	b.d.l.	94.734
Sphalerite	1	0.973	b.d.l.	b.d.l.	0.027	63.537	b.d.l.	b.d.l.	0.111	30.68	b.d.l.	b.d.l.	b.d.l.	b.d.l.	95.328

b.d.l.: below detection limit, low totals are due to the small size of the analyzed grain

ever, this type of pyrite contains more Au (up to 1500 ppm), than the framboidal one. According to the elemental mapping, Au and the other trace elements occur uniformly distributed in these pyrite crystals (Fig. 4).

In spite of the observed uniform Au distribution in the framboidal pyrite and in the euhedral overgrowths, it is possible, that Au is present not only as invisible gold in the pyrite structure, but also as nanosized free gold particles. The maximum Au concentration, which can be dissolved in the pyrite, depends on its As content according to the equation defined by REICH et al. (2005), and the measured Au content in the studied framboids is well above this limit.

Besides the aforementioned common opaque minerals, disseminated euhedral and anhedral pyrite (not forming aggregates or framboids), anhedral chalcopyrite, galena and sphalerite were also recorded (Fig. 2/2, 5, 6). They are mostly disseminated in the limestone, in some cases, occurring along the stylolites (Fig. 2/2) or within bedding. The disseminated euhedral pyrite is generally 5-20 μm in size, while the size of the anhedral crystals is 50-100 μm. With a few exceptions, chalcopyrite, sphalerite and galena form grains less than 10 μm in size. EPMA analyses of euhedral pyrite revealed a different composition from the two previously discussed pyrite types; it is characterized with high As (up to 2.065 mass%) and Pb (up to 0.335 mass%) content. Chalcopyrite is enriched in Au (up to 1200 ppm), and contains a small amount of Ag, Co, Ni and Zn (0.03–0.06 mass%). Due to their small size, few grains of sphalerite were quantitatively analyzed, and only one set of analyses is of good quality. It contains Cu, Pb and Fe as trace elements (0.027–0.973 mass%) (Table 1).

4.3. Geochemistry

Whole rock geochemical analyses were carried out on 3 samples, which are representative of the well studied section of the borehole (933.0 m, 950 m and 962.0 m). All the samples represent marly limestone with minor shale intercalations, though the carbonate-siliciclastic rock ratio was obviously slightly different.

The variable proportions of the carbonate, marl and shale in the samples is evident in the deviation of CaO content (18.3–36.1%) and SiO_2 content (22.3–57.6%). The 0.7–1.5 % Fe_2O_3 and MgO contents are controlled by the presence of Fe-bearing dolomite, although the Fe contribution of the pyrite has to be taken into consideration too (Table 2.).

The amount of Co, Cr, Cu, V, W and Zn exceeds the Clark-value of a typical limestone (LEVINSON, 1974), resulting in a characteristic 100-200 ppm total metal content (Table 2, Fig. 5). This result is much lower, than observations by BAKSA et al. (1981) from the same borehole. This could have been caused by the fact, that the two sampling methods were entirely different.

The samples are characterized by slightly higher Zr, Th, Hf, Ti, Y and As content in comparison to a typical limestone (LEVINSON 1974), caused by the presence of the accessory zircon, titanite, apatite and As-bearing pyrite, respectively (Table 2).

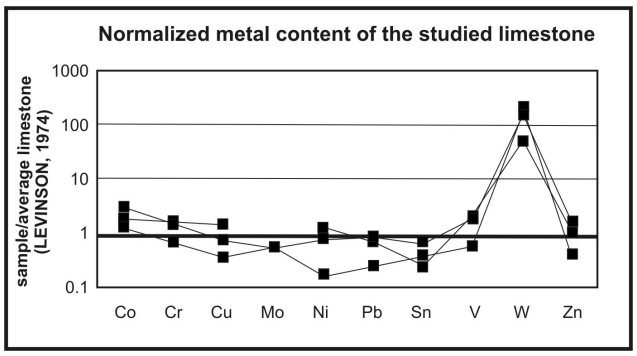

Figure 5: Normalized metal content of the studied limestone. A slight enrichment can be observed in the Co, Cr, Cu, Ni, V and Zn content, while W enrichment can be greater by a factor of 100 (samples are from 933 m, 950 m and 962 m).

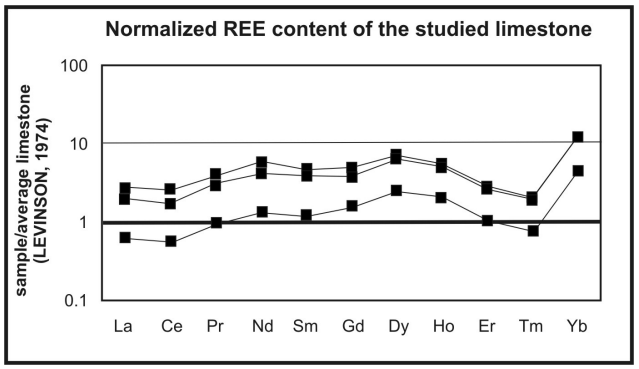

Figure 6: Normalized REE content of the studied limestone. In general, the samples are enriched in all the REEs, especially in Dy and Yb (samples are from 933 m, 950 m and 962 m).

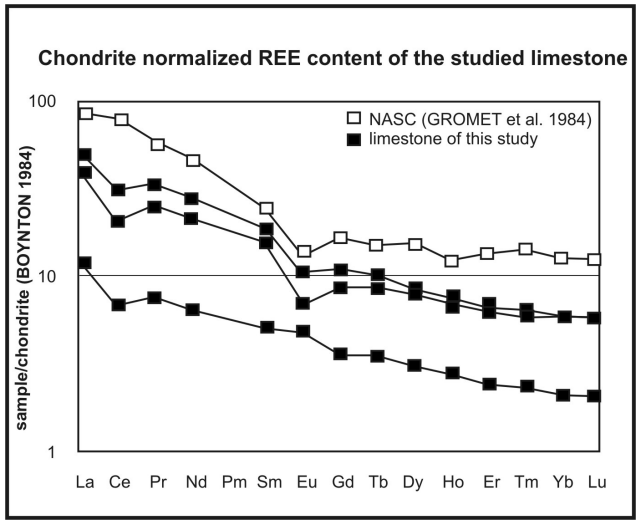

Figure 7: Chondrite normalized REE spider diagram of the studied limestone. As a comparison, North American shale composite (NASC) is plotted on the same diagram. The studied marly limestone shows significant similarities to that shale formed under anoxic conditions.

On average, the total rare earth element (REE) content of the analysed samples is 50 ppm (Table 2), which can be considered as an enrichment in relation to typical limestone (LEVINSON, 1974). If the results are normalized to the av-

Table 2: The results of the geochemical analyses.

Marly limestone			
	1	2	3
RM-131	933 m	950 m	962 m
Al_2O_3	3.64	3.65	0.983
BaO	0.009	0.012	<0.005
CaO	18.3	36.1	27.7
Fe_2O_3	1.06	1.56	0.702
K_2O	0.681	0.614	<0.20
MgO	1.08	1.29	0.628
MnO	0.113	0.157	0.118
Na_2O	0.128	0.542	<0.03
P_2O_5	<0.15	<0.15	<0.15
SiO_2	57.6	22.3	45.0
SO_3	0.206	<0.15	<0.15
SrO	0.036	0.070	0.056
TiO_2	0.136	0.170	0.041
results are given in %			
As	4.68	3.72	3.36
Cd	0.15	<0.1	<0.1
Cs	1.11	0.79	0.38
Hf	1.56	1.30	0.57
Nb	3.20	4.02	1.02
Rb	32.7	27.2	9.06
Ta	0.89	0.74	0.78
Th	2.51	2.79	0.71
Tl	0.16	<0.1	<0.1
U	0.82	0.51	0.37
Y	13.9	16.4	6.49
Zr	25.3	23.0	8.44
results are given in %			

Marly limestone			
	1	2	3
RM-131	933 m	950 m	962 m
Ag	<0.1	<0.1	<0.1
Au	*	*	*
Bi	<0.25	<0.25	<0.25
Co	11.3	7.42	4.91
Cr	15.2	15.6	6.26
Cu	10.1	20.2	5.17
Ir	<0.05	<0.05	<0.05
Mo	0.52	<0.25	0.57
Ni	9.21	15.0	2.09
Pb	6.05	5.48	1.92
Pd	<0.05	<0.05	<0.05
Pt	<0.05	<0.05	<0.05
Re	<0.05	<0.05	<0.05
Ru	<0.05	<0.05	<0.05
Sb	0.11	0.14	0.20
Sn	2.52	0.96	1.53
Te	<0.05	<0.05	<0.05
V	27.6	29.1	8.75
W	75.1	24.1	88.2
Zn	36.1	22.4	9.91
results are given in ppm			

Marly limestone			
	1	2	3
RM-131	933 m	950 m	962 m
La	12.2	16.2	3.76
Ce	16.8	25.4	5.53
Pr	3.07	4.11	0.93
Nd	12.7	16.9	3.88
Sm	3.06	3.68	0.98
Eu	0.51	0.76	0.35
Gd	2.24	2.82	0.93
Tb	0.41	0.48	0.17
Dy	2.56	2.74	1.00
Ho	0.49	0.54	0.20
Er	1.32	1.41	0.51
Tm	0.19	0.20	0.08
Yb	1.22	1.22	0.44
Lu	0.19	0.19	0.07
results are given in ppm			

erage REE composition of the limestone (LEVINSON 1974), all the REE display, with a few exceptions, a slight enrichment, with relatively high concentrations of Dy and Yb (Fig. 6.). The chondrite normalized REE diagram shows, that the investigated samples are enriched in all the REE, especially in the light ones (up to 10–100 times) (Fig. 7.). Two of the studied samples show significant similarities with each other, as well as with the North American shale composite (NASC, GROMET et al. 1984), which was plotted for comparison (discussion see below). However, the third analysis is characterized with less enrichment, but a similar pattern, except for the Eu value. This is probably caused by the different proportions of the rock forming and accessory minerals.

The concentrations of precious metals, such as Ag, Ir, Ru, Pt and Pd are always below the detection limit, while the measurement of Au was reported (Table 2.).

5. DISCUSSION

In the past, framboidal pyrite was thought to be able to form only during diagenesis, by biogenic processes. Since then, it has been recognised, that framboidal pyrite may also form during low temperature hydrothermal processes and low grade metamorphism (SCOTT et al. 2009 and references therein).

Our results show that framboidal pyrite of the studied marly limestone sequence is rich in trace elements and commonly it contains As, Cu, Co, Ni, but Au, Ag, Sb, Zn, Pb, Te

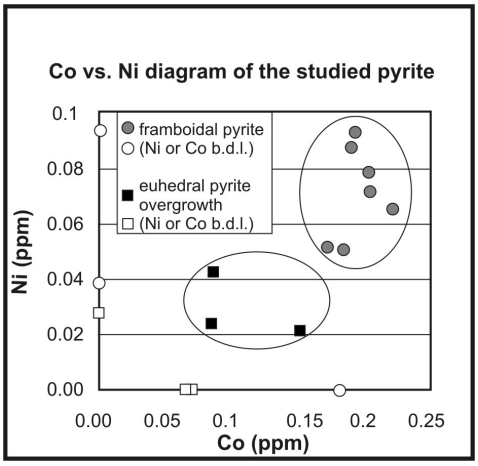

Figure 8: Comparison of the Ni and Co content of the studied framboidal pyrite and euhedral pyrite overgrowths. It can be clearly seen, that the two pyrite types are characterized by their different composition (empty squares and circles indicate the Co or Ni content of those crystals, where Ni or Co content was below the detection limit).

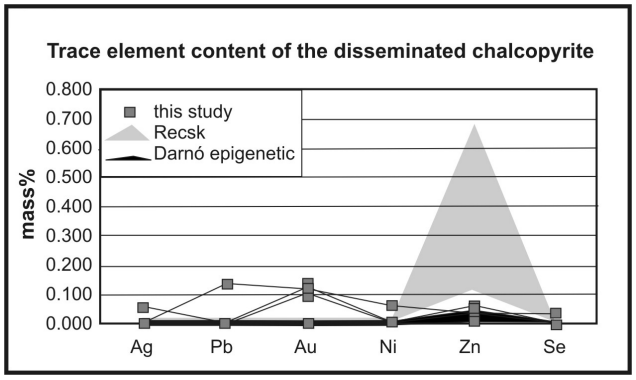

Figure 9: Trace element composition of the studied disseminated chalcopyrite, compared to the analyses of the nearby occurring chalcopyrite ore indications (analyses were carried out by the authors, for comparison purposes)

and Se. According to MITCHELL (1968), this set of trace elements is typical for those framboidal pyrites, which form during sedimentary processes. RAISWELL & PLANT (1980) and LARGE et al. (2009) also agreed with this statement. According to them, these trace elements commonly enrich in the upper part of the sediments, therefore, this local source can play an important role in the composition of the sedimentary pyrite.

In the investigated samples, the appearance of the euhedral pyrite aggregates postdates the framboidal pyrite formation. This can be well explained, if the formation criteria of the framboid development are taken into consideration. Highly supersaturated fluid is needed for framboidal pyrite formation, but the (pore) fluids can be exhausted rapidly, as Fe is very reactive (OHFUJI & RICKARD, 2005). Thus, after depleting the local (sedimentary) Fe source, transportation from an external source is needed (RAISWELL & PLANT, 1980). In conclusion, the transition from the framboidal to the euhedral pyrite aggregates can be interpreted to be a result of the change of the Fe source and the fluid. Another interpretation could be the recrystallisation of framboids to euhedral pyrite with the progress of diagenesis, as shown by PALINKAŠ (pers comm.) in the case of a lateritic crust in Croatia. However, the first option is more supported by the facts as the two pyrite types are characterized by different trace element composition (Fig. 8.). The euhedral overgrowths are generally less enriched in trace elements (except for the Au content), which is common in pyrite of hydrothermal or metamorphic origin. This change in the trace element content can be caused by several factors, including the metal content of the migrating fluid, or the ability of the trace elements to substitute in the pyrite structure. However, the larger, euhedral crystals were most probably formed more slowly and at higher temperatures than the framboidal pyrite, which can also be a very important factor. This results in a larger grain size, and pyrite crystals with less enriched trace element content. This is due to the fact, that the trace elements most likely partition into separate sulphide phases (e.g. sphalerite, galena, chalcopyrite), rather than become incorporated into the pyrite (LARGE et al., 2009).

Besides the framboidal and euhedral aggregate pyrite, several other sulphide phases were found in the studied drill core section including disseminated euhedral and anhedral pyrite (which do not form aggregates or framboids), anhedral chalcopyrite, sphalerite and galena.

The disseminated pyrite most probably formed from yet another fluid, as it has it's own different trace element content. However, in contrast to those pyrites, where no relation to any structure was observed, this pyrite type was often related to the stylolites. Thus, it can be concluded, that its formation was related to diagenetic processes.

The high Au content of the studied chalcopyrite grains seems to be typical of this occurrence. Though a few nearby localities contain chalcopyrite mineralization, none of them is characterized by a similar composition (Fig. 9.). The epigenetic chalcopyrite, which is found in quartz-prehnite veins of low grade metamorphic origin in Darnó Hill (MOLNÁR & KISS, 2013), contains only a few trace elements (e.g. low amount of Zn), while chalcopyrite formed in the Palaeogene Cu-porphyry-epithermal system of Recsk (located just 5 km W from the studied locality, see e.g. MOLNÁR, 2007 and the references therein) is characterized by it's typical high Zn content (0.1-0.7%). They can also be associated with gold, but lack the other trace elements, which are common in the studied drillcores. Therefore, these mineralizations formed under different conditions, although geographically they are located very close to each other. The latter statement was also proven by the composition of the framboidal pyrite. Framboidal pyrite was also found in the Lejtakna mineralization of the Recsk Ore Field, but it is characterized by a completely different trace element distribution (higher As, Pb and Zn and lower Co content in analyses undertaken for comparison purposes).

Based on the above discussed trace element distribution, the formation of the framboidal pyrite investigated in this contribution is related to sedimentary processes, while the euhedral pyrite overgrowths and the disseminated sulphides were formed by later fluid migration processes (most likely diagenetic, as no sign of hydrothermal processes was observed). These results allow establishment of more genetic models, as discussed below.

BAKSA et al. (1981) found, that the framboids found in the same unit formed most probably during a process similar to the *Kupferschiefer* formation. They came to this conclusion because of the observed synsedimentary (biogenic) characteristics and the stratigraphic position of the host rock. However, several characteristics observed by them were not discovered during our research (e.g. occurrence of the framboids parallel to the bedding, occurrence of the chalcopyrite rim along the margins of the framboids). Furthermore, several characteristics, typical of the *Kupferschiefer*, were not observed in our samples (e.g. Ag or PGE enrichment, occurrence of other characteristic copper minerals). The data presented in this work (e.g. the high Au content of the pyrite and the silica replacement of the carbonate), together with the framboid formation display some similarity with the Carlin-type Au (SCHROETER & POULSEN, 1996), though some important characteristics, like the presence of a very large leaching/alteration zone are missing. However, this option must be considered due to the proximity of the Recsk subvolcanic Cu-porphyry intrusion, especially because during a complex research programme, a Carlin-type Au indication was discovered 5 km north of Recsk (KORPÁS et al., 1999).

Recent results on the geology of Darnó Hill (KOVÁCS et al., 2008, KISS et al., 2010, 2012) have proven the occurrence of the Neotethyan rifting related environments in several blocks of the mélange, thus geologically the *Kupfershiefer* analogy seem to be a reasonable option. The recorded Co, Cr, Cu, V and Zn enrichment fit well into the geochemical signature of the *Kupferschiefer* mineralization (LEFEBURE & ALLDRICK, 1996), and differs significantly from the ones typical of the Carlin-type mineralization (SCHROETER & POULSEN 1996, STRMIĆ PALINKAŠ et al., 2010). The geochemical features of the investigated samples (together with the other observations, e.g. the mineral paragenesis, the presence of synsedimentary and early diagenetic processes) fit well with the characteristics of the weakly mineralized type of Kupfershiefer mineralization defined by VAUGHAN et al. (1989).

Only the W enrichment is not consistent with the *Kupferschiefer* mineralization. However, LARGE et al. (2011) listed W among the elements, that can be enriched during synsedimentary/early diagenetic processes. According to those authors, several trace elements, initially bonded with organic matter, can be enriched in organic rich muds, from which during synsedimentary/early diagenetic processes, they can partition into the growing pyrite or can form micro inclusions. Many of these elements, like Mo, V, U, Ni, Cr, As, and Cu are redox-sensitive, therefore their enrichment indicates a reducing, anoxic to euxin marine environment. This fact is also supported by the REE content of the investigated rock, as their amount and distribution is very similar to the North American anoxic shales (GROMET et al., 1984, Fig. 7). These observations suggest that the geological environment of the studied mineralization is very similar to the *Kupferschiefer* mineralization

Until now the presence of a weakly mineralized type of the black shale hosted ore mineralization (i.e. only the first mineralization stage) has been verified. The lack of the later stages (average mineralization, ore mineralization and post-diagenetic, structure controlled mineralization, VAUGHAN et al., 1989) can be explained by more models. On one hand, sufficient time is needed for generation of a *Kupferschiefer*-type deposit of economic importance (HITZMAN et al., 2010). If that was not available, then the development of the later mineralization stages was not possible. However, it is possible that any of the later stages developed, but their representatives are not found in the mélange, due to later tectonic processes, which formed the different units and the knappe system of the Bükk Mts.. Last but not least, as this mineralization was discovered ~1 km deep in the crust, in deep drillings, systematic exploration may lead to discovery of the later stages, either here in Darnó Hill, or at shallower parts of the same tectonic unit in the Bükk Mts. As *Kupferschiefer*-type mineralization is also known in the geologically correlated Dinarides (PALINKAŠ et al., 2008, 2014 in prep.), the latter two options seem to be more probable.

6. SUMMARY AND CONCLUSIONS

The study on the framboidal- and euhedral pyrite overgrowths within the marly limestone of the NE Hungarian Darnó Hill revealed that the rock contains disseminated chalcopyrite, sphalerite and galena.

The difference in the trace element composition of the two pyrite types is most probably caused by the difference in their formation processes. The high trace element content of the framboidal pyrite suggests that it formed during synsedimentary processes. In contrast, the euhedral aggregates could have formed from a later diagenetic fluid, concomitantly with chalcopyrite, sphalerite, and galena. Thus, at least two steps can be distinguished during the formation of the investigated mineralization.

Framboidal pyrite occurrence is known in the nearby Recsk Ore Field (Palaeogene epithermal and Cu-porphyry system, see e.g. MOLNÁR, 2007 and the references therein), but based on our results, the connection between the genesis of the two phenomena can be excluded. The observed mineral paragenesis, as well as the trace element content of the ore minerals and the whole rock analyses suggest that the investigated mineralization formed under reducing, anoxic marine conditions. The results presented here support the presence of a weakly mineralized, synsedimentary type black shale hosted base metal mineralization (VAUGHAN et al., 1989). The lack of the later mineralization stages could be the result of either a lack of time for the development of the ore forming processes, destruction by the later tectonic processes or simply requires further exploration.

ACKNOWLEDGEMENT

The authors wish to thank É. HARTAI for fruitful discussions.

The University Centrum for Applied Geosciences (UCAG) is thanked for access to the E. F. Stumpfl Electron Microprobe Laboratory.

The work was supported by the AÖU (Stiftung Aktion Österreich-Ungarn) research grant no. 85öu11 to G. KISS and F. ZACCARINI.

The described work was partly carried out as part of the TÁMOP-4.2.2.A-11/1/KONV -2012-0005 project as a work of Center of Excellence of Sustainable Resource Management, in the framework of the New Széchenyi Plan. The realization of this project is supported by the European Union, cofinanced by the European Social Fund.

REFERENCES

AIGNER-TORRES, M. & KOLLER, F. (1999): Nature of the magma source of the Szarvaskő complex (NE- Hungary).− Ofioliti, 24, 1–12.

BAKSA, CS., CSILLAG, J., DOBOSI, G. & FÖLDESSY, J. (1981): Rézpala indikáció a Darnó-hegyen (Copper shale indication on the Darnó Hill).− Földt. Közl., 111, 59–66 (in Hungarian with English abstract).

BOYNTON, W. V. (1984): Cosmochemistry of the rare earth elements: meteorite studies.– *In*: HENDERSON P. (ed.): Rare Earth Element Geochemistry. Elsevier, Amsterdam, 63–114

CSONTOS, L. (1995): Tertiary tectonic evolution of the Intra-Carpathian area: A rewiev.– Acta Vul., 7/2, 1–13.

CSONTOS, L. (1999): A Bükk-hegység szerkezetének főbb vonásai (Structure of the Bükk Mts.).− Földt Közl, 129/4, 611–651 (in Hungarian).

DIMITRIJEVIĆ, M. N., DIMITRIJEVIĆ, M. D., KARAMATA, S., SUDAR, M., GERZINA, N., KOVÁCS, S., DOSZTÁLY, L., GULÁCSI, Z., LESS, GY. & PELIKÁN, P. (2003): Olistostrome/mélanges – an overview of the problems and preliminary comparison of such formations in Yugoslavia and NE Hungary.− Slovak Geol Mag, 9/1, 3–21.

FÖLDESSY, J. (1975): Petrological study of a diabase-spilit magmatic rock suit, Darnó-hegy (Sirok, Hungary).− Proc. Xth Congr. CBGA 1973, 55–64.

GROMET, P. L., DYMEK R. F., HASKIN L. A. & KOROTEC R. L. (1984): The „North American shale composite": Its compilation, major and trace element characteristics. − Geochim et Cosmochim Acta, 48, 2469–2482.

HAAS, J. & KOVÁCS, S. (2001): The Dinaric-Alpine connection—as seen from Hungary.− Acta Geol Hung, 44/2–3, 345–362.

HAAS, J., KOVÁCS, S., PELIKÁN, P., KÖVÉR, SZ., GÖRÖG, Á., OZSVÁRT, P., JÓZSA, S. & NÉMETH, N. (2011): A Neotethys-óceán akkréciós komplexumának maradványai Észak-Magyarországon (Remnants of the Neotethyan accretionary complexes in N-Hungary).− Földt Közl, 141/2,167–196 (in Hungarian, with English abstract)

HAIDINGER, W. (1850): Note über das Vorkommen von gediegenem Kupfer zu Recsk bei Erlau in Ungarn.− Jahrb. der Geol. Reichsanstalt, I, 145–149.

HARANGI, SZ., SZABÓ, CS., JÓZSA, S., SZOLDÁN, ZS., ÁRVASÓS, E., BALLA, M. & KUBOVICS, I. (1996): Mesozoic igneous suites in Hungary: implications for genesis and tectonic settings in the Northwestern part of Tethys.− Int. Geol. Rev., 38, 336–360

HITZMAN, M. W., SELLEY, D. & BULL, S. (2010): Formation of Sedimentary Rock-Hosted Stratiform Copper Deposits through Earth History.− Econ. Geol., 105, 627–639.

KISS, G., MOLNÁR, F. & PALINKAŠ, L. A. (2008): Volcanic facies and hydrothermal processes in Triassic pillow basalts from the Darnó Unit, NE Hungary.− Geol. Croat., 61/2–3, 385–394.

KISS, G., MOLNÁR, F., †KOVÁCS, S. & PALINKAŠ, L. A. (2010): Field characteristics and petrography of the advanced rifting related Triassic submarine basaltic blocks in the Jurassic mélange of the Darnó Unit.− Centr. Eur. Geol., 53/2–3, 181–204.

KISS, G., MOLNÁR, F., PALINKAŠ, L. A., KOVÁCS, S. & HRVATOVIĆ, H. (2012): Correlation of Triassic advanced rifting related Neotethyan submarine basaltic volcanism of the Darnó Unit (NE Hungary) with some Dinaridic and Hellenidic occurrences on the basis of volcanological, fluid-rock interaction and geochemical characteristics.− Int. J. Earth Sci., 101/6, 1503–1521.

KISS, J. (1958): Ércföldtani vizsgálatok a Darnó-hegyen (Ore geological studies on the Darnó Hill).− Földt. Közl., 88, (in Hungarian).

KORPÁS, L. A., HOFSTRA, A., ÓDOR, L., HORVÁTH, I., HAAS, J. & ZELENKA, T. (1999): Evaluation of the prospected areas and formation. *In:* Carlin gold in Hungary.− Geol. Hung. Ser. Geol., 24, 197–293.

KOVÁCS, S., HAAS, J., SZEBÉNYI, G., GULÁCSI, Z., PELIKÁN, P., B.-ÁRGYELÁN, G., JÓZSA, S., GÖRÖG, Á., OZSVÁRT, P., GECSE, ZS. & SZABÓ, I. (2008): Permo-Mesozoic formations of the Recsk-Darnó Hill area: stratigraphy and structure of the pre-tertiary basement of the paleogene Recsk orefield. In: *Földessy J, Hartai É* (ed): Recsk and Lahóca Geology of the Paleogene ore complex. − Geosciences, Publications of the University of Miskolc, Series A, Mining, 73, 33–56.

†KOVÁCS, S., HAAS, J., OZSVÁRT, P., PALINKAŠ, L. A., KISS, G., MOLNÁR, F., JÓZSA, S. & KÖVÉR, SZ. (2010): Re-evaluation of the Mesozoic complexes of Darnó Hill (NE Hungary) and comparisons with Neotethyan accretionary complexes of the Dinarides and Hellenides – preliminary data.− Centr. Eur. Geol., 53/2-3, 205-231.

LARGE, R.R., BULL, S.W. & MASLENNIKOV, V.V. (2011): A Carbonaceous Sedimentary Source-Rock Model for Carlin-Type and Orogenic Gold Deposits.− Econ. Geol., 106, 331–358.

LARGE, R. R., DANYUSHEVSKY, L., HOLLIT, C., MASLENNIKOV, V., MEFFRE, S., GILBERT, S., BULL, S., SCOTT, R., EMSBO, P., THOMAS, H., SINGH, B. & FOSTER, J. (2009): Gold and trace element zonation in pyrite using a laser imaging technique: Implications for the timing of gold in orogenic and Carlin-style sediment-hosted deposits.− Econ. Geol., 104, 635–668.

LEFEBURE, D.V. & ALLDRICK, D.J. (1996): Sediment-hosted Cu+/-Ag+/-Co. *In:* LEFEBURE, D.V. & HÕY, T. (Eds): Selected British Columbia Mineral Deposit Profiles, Vol. 2 - Metallic Deposits. − British Columbia Ministry of Employment and Investment, Open File 1996-13, 13–16.

LEVINSON, A. A. (1974): Introduction to exploration geochemistry.– Calgary, Canada, Applied Publishing Ltd., 612 p.

MEZŐSI, J. & GRASSELLY, GY. (1949): A bajpataki (Mátra hgs.) természéz előfordulás (The occurrence of native copper in the Mátra Mountains at Bajpatak).− Acta Mineral., Petrogr., III, 44-47 (bilingual paper).

MITCHELL, R.M. (1968): A semi-quantitative study of trace elements in pyrite by spark source mass spectrography.− Norsk. Geol. Tidsskr., 48, 65–80.

MOLNÁR, F. (2007): The Cu-Au-Ag-Zn-Pb ore complex at Recsk: a uniquely preserved and explored porphyry-skarn-epithermal system. – Proceedings of the 9th Biannual SGA Meeting, Dublin, Ireland, 1: 226–240

MOLNÁR, ZS. & KISS, G. (2013): Study of the epigenetic copper occurrence of the Darnó Hill and its correlation with some Dinaridic and Hellenidic occurrences. Geoscience Meeting and Exhibition, Abstract book, ISBN: 978-693-8221-50-6

OHFUJI, H. & RICKARD, D. (2005): Experimental synthesis of framboids – a review.− Earth. Sci. Rev., 71, 147–170.

ORAVECZ, J. (1978): Az Rm-131-es sz. fúrás alaphegységi rétegsorának vizsgálata (Stratigraphical study of the Rm-131 drilling).− Eötvös Loránd University, Department of Geology, manuscript.

PALINKAŠ, L.A., BOROJEVIĆ ŠOŠTARIĆ, S. & STRMIĆ PALINKAŠ, S. (2008): Metallogeny of the Northwestern and Central Dinarides and Southern Tisia.− Ore Geol. Rev., 34, 501–520.

PALINKAŠ, L., MAVRIĆ, D., BERMANEC, V., FILIPOVIĆ, LJ. (2014): Copper mineralization within metadolomites in the Medvednica Mt., NW Croatia. (in prep.).

RAISWELL, R. & PLANT, J. (1980): The incorporation of trace elements into pyrite during diagenesis of black shales, Yorkshire, England. − Econ. Geol., 75, 684–699.

REICH, M., KESLER, S.E., UTSUNOMIYA, S., PALENIK, C. S., CHRYSSOULIS, S.L. & EWING, R. (2005): Solubility of gold in arsenian pyrite.− Geochem et Cosmochim Acta, 69, 2781–2796.

SCHMID, M. S., BERNOULLI, D., FÜGENSCHUH, B., MATENCO, L., SCHEFER, S., SCHUSTER, R., TISCHLER, M. & USTASZEWSKI, K. (2008): The Alpine-Carpathian-Dinaridic orogenic system: correlation and evolution of tectonic units.− Swiss J Geosci, 101/1, 139–183.

SCHROETER, T. & POULSEN, H. (1996): Carbonate-hosted Disseminated Au-Ag.– *In:* LEFEBURE D.V. & HÕY T. (eds): Selected British Columbia Mineral Deposit Profiles, Vol. 2 - Metallic Deposits. − British Columbia Ministry of Employment and Investment, Open File 1996-13, 9–12.

SCOTT, R. J., MEFFRE, S., WOODHEAD, J., GILBERT, S. E., BERRY, R. F. & EMSBO, P. (2009): Development of Framboidal Pyrite During Diagenesis, Low-Grade Regional Metamorphism and Hydrothermal Alteration.− Econ. Geol., 104, 1143–1168.

STRMIĆ PALINKAŠ, S., BOROJEVIĆ ŠOŠTARIĆ, S., PALINKAŠ, L., PECSKAY, Z., BOEV.B, BERMANEC, V. (2010): Fluid inclusions and K/Ar dating of the Allshar Au-Sb-As-Tl mineral deposit, Macedonia. Geol. Macedonica, 24/1, 63–71.

VAUGHAN, D. J., SWEENEY, M., FRIEDRICH, G., DIEDEL, R. & HARANCZYK, C. (1989): The *Kupferschiefer*: An Overview with an Appraisal of the Different Types of Mineralization.− Econ Geol, 84, 1003–1027.

Manuscript received February 08, 2013
Revised manuscript accepted September 26, 2013
Available online November 06, 2013